Journal of Magnetic Resonance **139,** 382–388 (1999)
Article ID jmre.1999.1795, available online at http://www.idealibrary.com on IDEAL®

# Magic Angle Spinning NMR Spectroscopy with Composite RF Pulses

Jörg Leppert, Bert Heise, and Ramadurai Ramachandran

*Abteilung für Molekulare Biophysik/NMR Spektroskopie, Institut für Molekulare Biotechnologie e.V., Postfach 100 813, D-07708 Jena, Germany*

Received January 26, 1999; revised April 20, 1999

**Using numerical optimization procedures it is shown that it is possible to design composite 180° RF pulses for MAS NMR spectroscopy by explicitly taking into account the variation of the resonance offset of each crystallite during the application of the RF pulses. When using composite RF pulses in experiments such as TOSS, where the delays between the RF pulses have to be critically adjusted, an optimization of these delays can lead to the desired performance characteristics.** © 1999 Academic Press

*Key Words:* **composite pulses; NMR; MAS; numerical optimization; TOSS.**

## INTRODUCTION

For the characterization of biomolecular structure and dynamics in polycrystalline or amorphous solids, with or without isotopic labeling, magic angle spinning (MAS) has become an invaluable tool (*1*). The lineshape of $^{1}$H decoupled, dilute spin-1/2 nuclei in solids is primarily governed by the chemical shift anisotropy (CSA) interaction, which can be an important source of structural information. When the spinning speed is less than the breadth of the static powder pattern, MAS breaks up the powder pattern into a sharp center band and a set of rotational sidebands. Principal values of the chemical shielding tensors can be obtained from an analysis of the sideband intensities. For each chemically inequivalent nucleus in the system, the spinning sidebands may span, depending upon the spinning speed, the entire range of the static powder pattern. In situations where this could possibly lead to overlapping sideband patterns that would make spectral analysis difficult, sidebands free MAS spectra can be generated by the TOSS sequence (*1–11*). In the interesting scenario wherein one needs both the isotropic and the anisotropic chemical shifts in polycrystalline samples having chemically inequivalent nuclei, one can achieve a complete resolution of isotropic and anisotropic chemical shifts via a two-dimensional approach employing TOSS sequences (*12*). Under MAS the structural informations contained in the weak homo- and heteronuclear dipolar couplings are normally lost. However, in the case of isotopically labeled biomolecules, the recent introduction of a plethora of powerful dipolar recoupling techniques for inhibiting the spatial averaging of weak dipolar couplings has enabled distance and torsion angle measurements under MAS (*13*). The efficacy of any multiple-pulse NMR sequence in generating satisfactorily the desired response from the system under investigation is critically dependent on the performance profile of the RF irradiations employed and MAS NMR is no exception to that. Multiple pulse MAS NMR experiments such as TOSS, PASS (*2*), etc., and many of the dipolar recoupling experiments mentioned above employ extensively multiple 180° pulses for both the inversion of longitudinal magnetization and the refocusing of transverse magnetization components. Obviously, the success of these experiments is critically dependent on the accuracy of these pulses. Composite RF pulses have found extensive usage in liquid state NMR in situations where the performance profile of a single RF pulse is not satisfactory, for example, due to its limited bandwidth. Composite RF pulses that have been developed for liquid state NMR applications can also be effectively employed, in principle, in MAS experiments (*14, 15*), in situations where the composite pulse durations are short enough with respect to the rotor period so that the variation in the resonance offset of each crystallite during the RF pulses can be neglected. Unfortunately, many of the short duration solution state composite 180° pulses do not have the desired performance profile and to date no composite pulses have been designed that explicitly take into account the effects of MAS during the pulses. It is conceivable that, even if they had been specifically constructed for solid state MAS applications, the mere incorporation of composite RF pulses in multiple pulse MAS experiments can lead to a poorer performance compared to that seen with the application of normal 180° pulses if the functioning of such sequences is also critically dependent on the interpulse durations, as in the case of TOSS. If long pulses are used then a significant portion of the critical free evolution times required between the RF pulses in such experiments will be occupied by the RF pulses themselves. In view of the potential of MAS NMR spectroscopy in the study of biomolecules, we are currently exploring the efficacy of numerical optimization procedures for the design of efficient RF irradiation schemes for MAS applications. The power of numerical optimization schemes has already been exploited in diverse fields of NMR research (*16–24*). Our exploratory theoretical studies, as described below, clearly indicate for the first time that it may be possible via such an approach to develop composite 180° pulses for MAS applications and to reoptimize



1090-7807/99 $30.00

the intercomposite pulse delays in experiments such as TOSS to obtain better performance characteristics than otherwise possible.

## DESIGN OF COMPOSITE PULSES FOR MAS NMR

In our approach, we consider an ensemble of spin-1/2 nuclei for which the MAS Hamiltonian in the rotating frame is given by (*4, 6*)

$$H(t) = -\Delta\omega I_z - \omega[\, g_1\cos(\omega_r t + \varnothing_1) + g_2\cos(2\omega_r t + \varnothing_2)]I_z, \quad [1]$$

where

$$\Delta\omega = [\tfrac{1}{3}\omega_0(\sigma_{11} + \sigma_{22} + \sigma_{33}) + \omega_{\text{off}}],$$

$$\omega = \omega_0[\sigma_{33} - \tfrac{1}{3}(\sigma_{11} + \sigma_{22} + \sigma_{33})],$$

$$g_1 = \tfrac{1}{2}\sin(2\theta_m)\sin\beta[(\eta\cos 2\gamma + 3)^2\cos^2\beta + \eta^2\sin^2 2\gamma]^{1/2},$$

$$g_2 = \tfrac{1}{2}\sin^2\theta_m[(\tfrac{3}{2}\sin^2\beta - \tfrac{\eta}{2}\cos 2\gamma\,(1+\cos^2\beta))^2 + \eta^2\cos^2\beta\sin^2 2\gamma]^{1/2},$$

$$\phi_1 = \alpha + \psi_1,$$

and

$$\phi_2 = 2\alpha + \psi_2.$$

In the above equation $\psi_1$, $\psi_2$, and $\eta$ are defined as

$$\tan\psi_1 = \frac{\eta\sin 2\gamma}{\cos\beta[\eta\cos 2\gamma + 3]}$$

$$\tan\psi_2 = \frac{-\eta\cos\beta\sin 2\gamma}{\tfrac{3}{2}\sin^2\beta - \tfrac{\eta}{2}\cos 2\gamma(1+\cos^2\beta)}$$

and

$$\eta = \frac{\sigma_{22} - \sigma_{11}}{\sigma_{33} - \tfrac{1}{3}\,\text{Tr}(\sigma)}.$$

($\alpha$, $\beta$, $\gamma$) are the Euler angles defining the orientation of the CSA tensor in the rotor frame, ($\sigma_{11}$, $\sigma_{22}$, $\sigma_{33}$) are the principal values of the CSA tensor, $\omega_0$ is the Larmor frequency, $\theta_m$ is the magic angle, and $\omega_{\text{off}}$ is the resonance offset. In the construction of a composite 180° RF pulse for MAS applications, the pulse widths ($\theta_1$, $\theta_2$, $\theta_3$, . . . , $\theta_N$) and phases ($\varphi_1$, $\varphi_2$, $\varphi_3$, . . . , $\varphi_N$) of the constituent pulses of the composite RF pulse are optimized via the simulated annealing optimization procedure (*25, 26*), so as to minimize the error function defined by

$$\epsilon(X) = \sum_{\alpha,\beta,\gamma} W_{\alpha\beta\gamma} \sum_{m,n}[U^{I}_{mn}(\theta,\varphi) - U^{CP}_{mn}(X,\, \omega_r,\, a,\, b)]^2, \quad [2]$$

where $X$ represents the $2N$ dimensional vector ($\theta_1$, $\theta_2$, . . . , $\theta_N$, $\phi_1$, $\phi_2$, . . . , $\phi_N$), $\omega_r$ the MAS frequency, and $U^{I}_{mn}$ the ($mn$) matrix element of an ideal propagator corresponding to a single 180° pulse with an RF field strength of $\omega_1^0$, phase of $\varphi$, and flip angle of $\theta$. $U^{CP}_{mn}$ represents the ($mn$) matrix elements of the propagator corresponding to the composite pulse sequence. $W_{\alpha\beta\gamma}$ is the probability of finding a crystallite at the orientation ($\alpha$, $\beta$, $\gamma$); $a$ and $b$ represent the normalized resonance offset ($\Delta\omega/\omega_1^0$) and RF field strength ($\omega_1/\omega_1^0$).

In our initial studies reported here we have assumed $\Delta\omega$ and $\eta$ to be zero. In the calculations of the time evolution operator during the application of the composite pulses we divide the composite pulses into a large number of small steps (10°) and assume that the time dependence of the Hamiltonian [1] can be neglected on the time scale of each step. That is, the resonance offset is assumed to vary only from one time segment to another and not during the individual time steps. The total time evolution operator for the entire pulse is then calculated by a time-ordered product of the time evolution operators corresponding to the individual time steps that constitute the composite pulse. Typically, we have considered 64 * 64 crystallite orientations for $\eta = 0$ case (64 * 64 * 64 for $\eta \neq 0$ case) in our calculations and we have neglected $H_1$ inhomogeneity effects and fluctuations in the spinning speed. While using composite pulses it is possible, wherever needed, to reoptimize intercomposite pulse delays to obtain the desired performance characteristics. For example, as will be shown below, it is possible to reoptimize intercomposite pulse delays in a TOSS sequence to achieve better sideband suppression than is otherwise possible.

## TOSS WITH COMPOSITE PULSES

TOSS involves the application of rotor synchronized 180° pulses with specific interpulse timings and the efficacy of the TOSS sequence in generating sidebands free MAS spectra is critically dependent on accurate 180° pulses and interpulse delays. To obtain optimal TOSS delays while using composite pulses, we assume once again an axially symmetric CSA tensor. Under this assumption it is seen from an analysis of the magnetization trajectories that TOSS leads to an alignment of the time-averaged magnetization vector of each crystallite. This leads to a situation where the centerbands of the subspectra of each crystallite are in phase while the sideband phases are such that the sidebands are cancelled under powder averaging. After a 90° pulse at $t = 0$, the magnetization vector associated with each crystallite, in a normal MAS experiment, accumulates a time-dependent phase that is governed by the

**TABLE 1**
**Composite Inversion Pulses for MAS Spectroscopy (Bandwidth = ($\pm 0.25\ \gamma H_1$), $\gamma H_1$ = 31.25 kHz)**

| MAS frequency (Hz) | Total composite pulse length (degrees) | Sequence |
|---|---|---|
| 1000 | 412.0 | $(59.1)_{188.9}(56.4)_{6.3}(90.5)_{2.6}(90.5)_{-2.6}(56.4)_{-6.3}(59.1)_{-188.9}$ |
| 1000 | 997.2 | $(215.3)_{145.2}(167.7)_{179.0}(231.2)_{66.3}(167.7)_{179.0}(215.3)_{145.2}$ |
| 3000 | 619.6 | $(53.1)_{204.2}(235.5)_{190.1}(21.2)_{10.7}(21.2)_{-10.7}(235.5)_{-190.1}(53.1)_{-204.2}$ |
| 3000 | 420.0 | $(60.0)_{180.0}(300.0)_{0.0}(60.0)_{180.0}$ |
| 5000 | 567.4 | $(171.0)_{185.9}(95.3)_{177.8}(17.4)_{91.5}(17.4)_{-91.5}(95.3)_{-177.8}(171.0)_{-185.9}$ |
| 5000 | 566.6 | $(156.2)_{186.4}(113.5)_{179.1}(13.6)_{76.1}(13.6)_{-76.1}(113.5)_{-179.1}(156.2)_{-186.4}$ |

Hamiltonian given above [1]. The phase angle at a time $t$ after the 90° pulse, under the assumption that the isotropic chemical shift is on resonance, is given by (*4, 6*)

$$\Phi(t) = \Omega_1\sin(\omega_r + \phi_1) + \Omega_2\sin(2\omega_r + \phi_2) - \Omega_1\sin\phi_1 - \Omega_2\sin\phi_2, \quad [3]$$

where $\Omega_1 = \omega g_1/\omega_r$ and $\Omega_2 = \omega g_2/2\omega_r$.

The average phase angle over one rotor period is given by

$$\theta_{av} = -\Omega_1\sin\phi_1 - \Omega_2\sin\phi_2. \quad [4]$$

The application of the rotor synchronized 180° pulses with specific interpulse delays in an ideal TOSS experiment affects the magnetization trajectories such that sidebands free spectra are generated. In particular, for the axially symmetric case it is seen that the average phase angle of the magnetization vectors for each crystallite, over one rotor period and starting from the point of data acquisition, becomes zero and results in the alignment of magnetization vectors of each crystallite along the $x$-axis (*4, 6, 11*). The critical condition to be fulfilled for achieving effective suppression of sidebands in a TOSS experiment while employing composite 180° RF pulses is that the interpulse delays have to be readjusted such that the initial phase of the magnetization vectors of each crystallite should satisfy the condition (*6*)

$$\Phi(0) = \Omega_1\sin\phi_1 + \Omega_2\sin\phi_2. \quad [5]$$

In our approach, we do a density matrix calculation of the evolution of the magnetization vectors for many crystallite orientations under MAS and employ numerical procedures to readjust the intercomposite pulse delays in a TOSS sequence. We optimize the intercomposite pulse delays by minimizing the error function given by

$$\Delta\epsilon(\tau_1, \tau_2, \ldots, \tau_n, \omega_r) = \sum_{\alpha,\beta,\gamma} W_{\alpha\beta\gamma}[\Phi^I(0) - \Phi^{CP}(0)]^2, \quad [6]$$

where $\tau_1, \tau_2, \ldots, \tau_n$ are the TOSS delays and $\Phi^{CP}(0)$ and $\Phi^I(0)$ represent, respectively, the initial phases calculated for the TOSS sequence employing the composite pulses and ideal 180° RF pulses. The calculation of the time evolution operator during the application of the composite pulses is carried out as before. The error function given in Eq. [6] can be minimized, depending on the situation, either via local or global numerical optimization procedures (*26*). While the first approach will be fast and work in situations where the starting point in the parameter space to be searched is close to a minimum in the error surface, the latter approach, although it may be time consuming, will lead to a global minimum, if such a solution indeed exists, irrespective of the initial point of search chosen in the parameter space. We have employed the Nelder–Mead simplex and the simulated annealing algorithms (*26*) for the local and global optimization, respectively. Only in situations where we find that possible starting points for a local optimization search do not lead to a good solution do we employ the global minimization procedure. Since in general global optimization carried out in a finite amount of time may not lead to the exact minimum in the error surface, we use the solutions obtained from the global optimization as a starting point for further improvement via a local optimization scheme. In this initial study such calculations have been carried out assuming once again ideal experimental conditions to minimize the computational time needed in the global minimization search. Typically, we consider an axially symmetric case and (8 * 8) crystallite orientations for calculating the optimal TOSS intercomposite pulse delays. For the local optimization calculations we have used as a starting point some of the solutions that have been reported by Lang (*8*) for a four-pulse TOSS sequence.

## RESULTS

In our calculations, we have considered typical MAS spinning speeds of 1, 3, and 5 kHz, CSA principal tensor elements of $\sigma_{11}$ = 5 ppm, $\sigma_{22}$ = 5 ppm, $\sigma_{33}$ = 130 ppm, an inversion bandwidth of $\pm 0.25\ \gamma H_1$, and a RF field strength corresponding to a 90° pulsewidth of 8 $\mu$s. In Table 1 we give some typical examples of composite 180° RF pulses obtained from the numerical optimization procedures outlined above. In Ta-

**TABLE 2**
**Normal (*8*) and Reoptimized Time Delays for a Four-Pulse TOSS Sequence[a]**

| $\nu_r$ (Hz) | $t_1$ | $t_2$ | $t_3$ | $t_4$ | $t_{acq}$ |
|---|---|---|---|---|---|
| For all $\nu_r$ (*8*) | 0.188821 | 1.230053 | 1.811179 | 2.769947 | 4.000000 |
| 1000 | 0.182689 | 1.225854 | 1.816961 | 2.773808 | 4.000025 |
| 3000 | 0.187054 | 1.229092 | 1.812186 | 2.770184 | 4.000071 |
| 5000[b] | 0.182134 | 1.011788 | 1.795181 | 2.519675 | 3.108296 |

[a] Time delays are expressed as a fraction of the rotor period. The reoptimized delays were obtained for the composite pulses given in Table 1 and with the durations of 997.2, 420.0, and 567.4°.
[b] Solution obtained via simulated annealing.

ble 2 we give, for a few cases, the optimized intercomposite pulse delays, with composite pulses replacing the ideal 180° RF pulses in the four-pulse TOSS sequence (*8*). Using the method outlined here and employing a SGI Power Challenge L (R10000), it takes approximately 50 h for the generation of a composite 180° pulse. It takes less than 10 min of CPU time to obtain optimized TOSS delays via the local and 15 h via the global optimization scheme. The typical responses of an ensemble of spin-1/2 nuclei to the composite inversion pulse and the composite pulse TOSS sequences are shown in Figs. 1 and 2, respectively. From Fig. 1 it is seen that the inversion profile of the composite RF pulse reported here is satisfactory in comparison to the response seen after a simple 180° or a $90_y180_x90_y$ composite pulse. Figure 2 demonstrates that TOSS spectra with good sideband suppression can be obtained by reoptimizing the intercomposite pulse delays. The composite pulses given in Table 1 are typical examples of sequences with reasonably satisfactory performance characteristics and which have been derived by putting some symmetry restrictions on the parameters of the component pulses so as to reduce the number of variables in the optimization procedure. We have also derived sequences without any restrictions and also

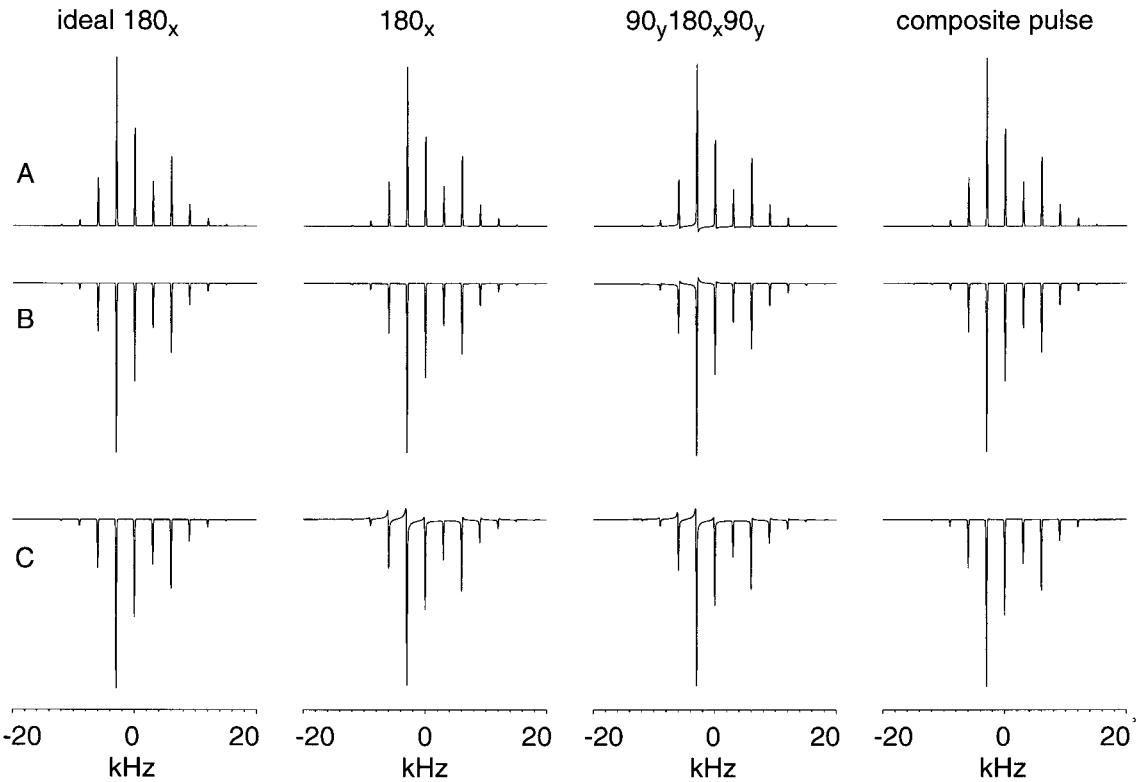


**FIG. 1.** Simulated MAS plots ($\nu_r$ = 3 kHz, $\omega_0$ = 125 MHz) of $\langle I_x \rangle$ (A), $\langle I_y \rangle$ (B), and $\langle I_z \rangle$ (C) following the inversion pulses indicated and starting from the thermal equilibrium density matrix $\rho(0) = I_x, I_y, I_z$, respectively. A RF field strength of 31.25 kHz and CSA parameters of $\sigma_{11}$ = 5 ppm, $\sigma_{22}$ = 5 ppm, and $\sigma_{33}$ = 130 ppm were employed in the simulations. The composite pulse $(53.1)_{204.2}(235.5)_{190.1}(21.2)_{10.7}(21.2)_{-10.7}(235.5)_{-190.1}(53.1)_{-204.2}$ was employed in the simulations shown in the last column.

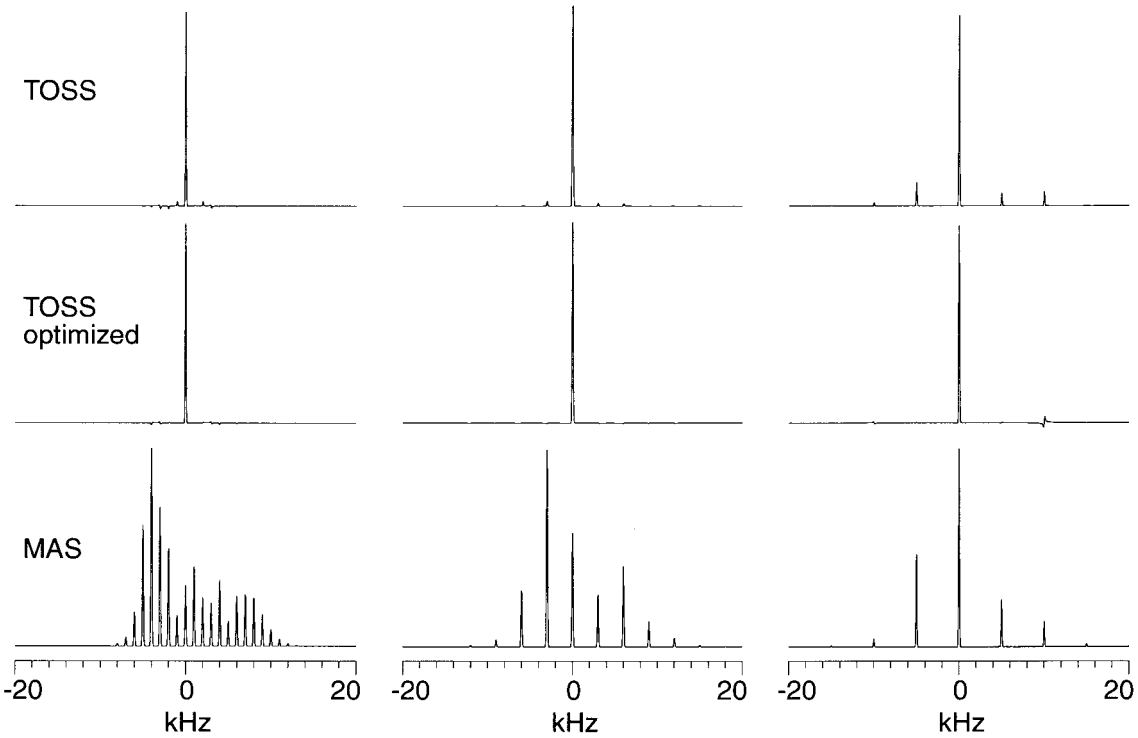


**FIG. 2.** Simulated MAS (ideal) and TOSS spectra obtained at $\nu_r = 1$, 3, and 5 kHz employing the CSA parameters of $\sigma_{11} = 5$ ppm, $\sigma_{22} = 5$ ppm, and $\sigma_{33} = 130$ ppm and a Larmor frequency of 125 MHz. The TOSS responses were obtained employing the intercomposite pulse delays given in Table 2 and the corresponding composite pulses. TOSS simulations were performed employing a RF field strength of 31.25 kHz. Wherever needed, addition of a whole number of rotor periods was effected to the intercomposite pulse delays. All interpulse delays are calculated from center to center of the RF pulses employed.

with RF pulse frequencies as an additional variable. However, our preliminary studies indicate that neither the total duration of the composite pulses nor the performance profiles get dramatically improved under these conditions. In the course of the TOSS intercomposite pulse delay optimization, we have also seen that satisfactory TOSS sideband suppression can be achieved in many cases where the inversion profile of the composite pulse sandwich is not ideal. In some situations it is seen that good TOSS performance can be obtained with normal TOSS delays. For example at $\nu_r = 1$ kHz the composite pulse given in Table 1 and with the total duration of 412° required no reoptimization of TOSS delays. On the other hand, sometimes the performance of the composite pulse TOSS sequences is not satisfactory even after optimizing the intercomposite pulse delays, although the inversion profiles of the composite pulses employed were satisfactory. It is conceivable that a proper approach for achieving good sideband suppression in TOSS experiments would involve the design of TOSS sequences per se. Such a process would necessarily entail more computational time. However, the fact that we are able to obtain improved sideband suppression by a reoptimization of the intercomposite pulse delays via the method outlined above offers support to the validity of the analysis of TOSS in terms of the alignment of magnetization trajectories (*4, 6, 11*). Although we have assumed an axially symmetric CSA tensor, to simplify the calculations, this does not preclude the applicability of the results reported here for $\eta \neq 0$ cases.

We have made an initial experimental assessment of the performance characteristics of the composite pulses reported here. Figure 3A shows normal 125-MHz CPMAS spectra of $^{13}C'$ ($\eta \neq 0$) in the peptide bond of the dipeptide Fmoc-($^{13}C'$,$^{15}N$)Aib-($^{15}N$)Aib$^{(1)}$-$NH_2$, which is under investigation in our laboratory. Figure 3B shows the spectra obtained after inverting the transverse magnetization following the cross polarization by the composite pulses indicated in the legend. Although the spectral range to be covered is larger than the bandwidth for which the composite pulses have been constructed, from Fig. 3B it is seen that the inversion profiles of the composite pulses are satisfactory. For minor variations in RF pulse flip angles, phases, and spinning frequencies it is seen from both numerical and experimental studies that the performance characteristics of the sequences are not very much affected, although they don't reach the full inversion efficiency of a 180° pulse. The spectra shown in Fig. 3 were recorded at room temperature employing a Varian $^{UNITY}$INOVA 500 MHz wide bore solid state spectrometer equipped with a 5-mm supersonic DOTY triple resonance probe. Fast small-angle phase shifts needed for the generation of composite pulses

[1] $\alpha$-Aminoisobutyric acid.

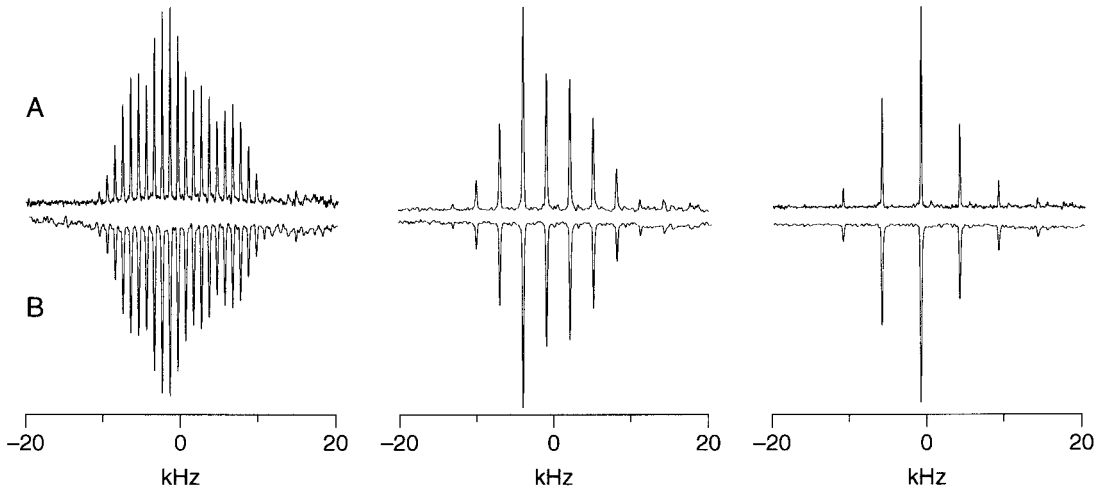


**FIG. 3.** (A) Experimental $^{13}C'$ CPMAS spectra ($\nu_r$ = 1, 3, and 5 kHz; $\sigma_{11}$ = 69, $\sigma_{22}$ = 77, $\sigma_{33}$ = 218 ppm) of the dipeptide and (B) the spectra obtained after inverting the transverse magnetization following the cross polarization by the composite pulses with durations of 997.2, 619.6, and 567.4° as given in Table 1. A RF field strength of 31.25 kHz was employed uniformly in all the three cases.

were achieved by employing the optional waveform generator in the spectrometer hardware.

## CONCLUSIONS

The present work clearly indicates the potential of numerical techniques in the design of efficient RF irradiation schemes needed for MAS applications. One of the main drawbacks of NMR is the poor inherent sensitivity of the technique and, hence, any means by which improvements in the signal-to-noise ratio (SNR) can be effected will have considerable impact on the general applicability of MAS NMR experiments in structural studies. Although novel ways for achieving this are currently being explored (*27, 28*), modest improvements in SNR can be easily obtained in principle by carrying out experiments at higher magnetic field strengths and/or with larger sample volumes, where possible. However, both situations can impose considerable demand on the requirements of the RF transmitters employed for achieving uniform excitation over the spectral range of interest. Under the circumstances where RF transmitter hardware requirements cannot be met satisfactorily, it is conceivable that the availability of composite pulses specifically tailored for MAS will have a dramatic impact on MAS NMR spectroscopy. The usage of large sample volumes may also require that one has to take into account $H_1$ inhomogeneity effects in the design of RF irradiation schemes. In this preliminary study, to reduce computational time, we have assumed ideal experimental conditions and neglected $H_1$ inhomogeneity effects, spinning speed fluctuations, distribution in isotropic chemical shifts, etc. The composite 180° pulses and optimized composite pulse TOSS delays have also been obtained for specific MAS frequencies and RF field strengths and this may limit the potential utility of the results reported here. The sequences reported in this work may not represent the ultimate inversion sequences for MAS experiments. However, it is shown here that composite pulses, although their durations can be considerably larger than a simple 180° pulse, can still be designed to provide satisfactory spin inversion. Encouraged by this, further works directed toward the generation of composite RF pulses are planned that will have convenient and direct applicability in routine experimental MAS NMR investigations and an assessment of the relative efficacy of different optimization schemes for increasing the speed of the computational process.

## REFERENCES


1. K. Schmidt-Rohr and H. W. Spiess, "Multidimensional Solid-State NMR and Polymers," Academic Press, London (1994).
2. W. T. Dixon, *J. Chem. Phys.* **77,** 1800 (1982).
3. W. T. Dixon, J. Schaeffer, M. D. Sefcik, E. O. Stejskal, and R. A. McKay, *J. Magn. Reson.* **49,** 341 (1982).
4. E. T. Olejniczak, S. Vega, and R. G. Griffin, *J. Chem. Phys.* **81,** 4804 (1984).
5. D. P. Raleigh, E. T. Olejniczak, S. Vega, and R. G. Griffin, *J. Magn. Reson.* **72,** 238 (1987).
6. D. P. Raleigh, E. T. Olejniczak, and R. G. Griffin, *J. Chem. Phys.* **89,** 1333 (1988)
7. D. P. Raleigh, E. T. Olejniczak, and R. G. Griffin, *J. Magn. Reson.* **93,** 472 (1991).
8. S. J. Lang, *J. Magn. Reson.* A **104,** 345 (1993).
9. Z. Song, O. N. Antzutkin, X. Feng, and M. H. Levitt, *Solid State Nucl. Magn. Reson.* **2,** 143 (1993).
10. O. N. Antzutkin, Z. Song, X. Feng, and M. H. Levitt, *J. Chem. Phys.* **100,** 130 (1994).
11. C. M. Rienstra, S. Vega, and R. G. Griffin, *J. Magn. Reson.* A **119,** 256 (1996).
12. A. C. Kolbert and R. G. Griffin, *Chem. Phys. Lett.* **166,** 87 (1990).
13. R. G. Griffin, *Nat. Struct. Biol.* **5,** 508 (1998).

*14.* D. P. Raleigh, A. C. Kolbert, and R. G. Griffin, *J. Magn. Reson.* **89,** 1 (1990).
*15.* A. Hagemeyer, D. Van der Putten, and H. W. Spiess, *J. Magn. Reson.* **92,** 628 (1991).
*16.* C. J. Hardy, P. A. Bottomley, M. O'Donnell, and P. Roemer, *J. Magn. Reson.* **77,** 233 (1988).
*17.* H. Geen and R. Freeman, *J. Magn. Reson.* **93,** 93 (1991).
*18.* F. S. Digennaro and D. Cowburn, *J. Magn. Reson.* **96,** 582 (1992)
*19.* V. Smith, J. Kurhanewicz and T. L. James, *J. Magn. Reson.* **96,** 345 (1992).
*20.* N. Sunitha Bai, M. Ramakrishna, and R. Ramachandran, *J. Magn. Reson.* A **102,** 235 (1993).
*21.* N. Sunitha Bai, M. Ramakrishna, and R. Ramachandran, *J. Magn. Reson.* A **104,** 203 (1993).
*22.* N. Sunitha Bai and R. Ramachandran, *J. Magn. Reson.* A **105,** 298 (1993).
*23.* N. Sunitha Bai, N. Hari, and R. Ramachandran, *J. Magn. Reson.* A **106,** 248 (1994).
*24.* K. Scheffler, *J. Magn. Reson.* B **109,** 175 (1995).
*25.* S. Kirkpatrick, C. D. Gelatt, and M. P. Vecchi, *Science* **220,** 671 (1983).
*26.* W. H. Press, B. P. Flannery, S. A. Teukolsky, and W. T. Vetterling, "Numerical Recipies: The Art Of Scientific Computing," Cambridge Univ. Press, Cambridge (1986).
*27.* R. Tycko, *Solid State Nucl. Magn. Reson.* **11,** 1 (1998).
*28.* G. J. Gerfen, L. R. Becerra, D. A. Hall, D. J. Singel, and R. G. Griffin, *J. Chem. Phys.* **102,** 9494 (1995).